Bol. Soc. Paran. Mat.
©SPM – E-ISSN-2175-1188
SPM: www.spm.uem.br/bspm

(3s.) **v. 2025 (43) 2** : 1–16.
ISSN-0037-8712
doi:10.5269/bspm.77367

A Computational Investigation of a Non-Singular Fractional Operator for an Unsteady MHD Flow Problem

Bhaskar Jyoti Bhuyan, Utpal Kumar Saha*, G. C. Hazarika and Dipen Saikia

ABSTRACT: This paper analyzes the impacts of thermal conductivity and variable viscosity on unsteady magnetohydrodynamic (MHD) fluid flow over an infinite vertical plate embedded in a porous medium, including thermal diffusion effects. Atangana–Baleanu (AB) and Caputo–Fabrizio (CF) fractional derivatives are applied in this work to model the system, including the effects of nonlocal and nonsingular kernels. A dimensionless formulation of the governing partial differential equations (PDEs) has been established. The equations are then discretized by using the ordinary finite difference approach and then numerically solved by adopting the Gauss-Seidel iteration process. The influences of different parameters involved in the problems have been illustrated graphically and numerically. The variation of AB and CF fractional derivatives is obtained through a MATLAB-based computational approach for the different values of velocity, temperature, and concentration distributions with respect to time under various parameters. A tabular comparison between AB and CF methods have been shown. It has been found that both approaches exhibit a significant level of consistency.

Key Words: Variable viscosity, thermal Conductivity, sorret effect, porous media, AB and CF fractional derivatives.

Contents

1. Introduction

Applications of the MHD principle can be found across several domains, such as plasma physics, astrophysics, missile technology, cosmology, and space technology. Recently, numerous researchers have concentrated on investigating the application of MHD flow fluid in porous media. The new trends in modern science and technology related to MHD have been profoundly shaped by the contributions of the great researchers cited in [1,2,3]. Nield and Bejan [4] thoroughly described the application of

* Corresponding author

Submitted June 18, 2025. Published August 12, 2025
2010 *Mathematics Subject Classification:* 76W05, 35R11, 65M06, 65M12, 26A33 .

fluid mechanics and heat transfer, including recent advancements in various fields of modern science and technology and also provided a detailed analysis of convective thermal energy transfer. The study mentioned in [5] examines how free convection currents influence the oscillatory flow of a polar fluid with a vertical plane boundary at constant temperature and focuses on the influence of various parameters on both velocity and angular velocity. The investigation explained in [6,7,8,9] focuses on the unsteady MHD flow of a Casson fluid flow past with different plates through a porous medium in presence of thermal radiation, chemical reaction effects, and heat source/sink. The research presented in [10,11,12,13,14] examined the impacts of thermal radiation, chemical reactions, and magnetic fields on the heat and mass transfer behavior of both unsteady and steady MHD flows in various fluid patterns, such as blood flow in porous vessels and hybrid nanofluids over permeable surfaces. O. Aydın and A. Kaya [15] conducted a study on mixed convection heat transfer around a permeable vertical plate. They focused on how magnetic fields and thermal radiation influence the process. In the studies cited in [16,17], the authors explored the combined impacts of radiation and rotation on the unsteady hydromagnetic free convection flow of a viscous incompressible and electrically conducting fluid. A. Kumar [18] studied MHD free convective fluctuating flow via porous media with variable permeability. The researchers in [19,20,21] performed a comprehensive examination of the effects of heat and mass transfer on the free convective rotational flow of a viscoelastic, incompressible and electrically conducting fluid. In [22,23,24,25], researchers examined how thermal radiation and mass transfer affects the MHD free convection flow. Their investigation evaluated flow via an exponentially accelerated vertical plate in a porous medium with the effects of variable temperature and concentration. The research conducted by [26,27] focused on the influences of magnetic hydrodynamics and scattering on fluid flow past an accelerated vertical plate in a porous medium with variable thermal diffusion. It also examines the impact of heat sources and radiation absorption on MHD fluid flow over an infinite vertical plate in the presence of the Soret effect. A detailed study on the effects of thermal diffusion on MHD flow past a semi-infinite exponentially accelerated vertical plate across porous medium can be seen in [28]. A comprehensive study on the unsteady MHD flow fluids over an inclined plate that is exponentially accelerated and embedded in a porous medium with variable thermal conductivity and the presence of radiation was investigated by S.F. Ahmmed et al. [29]. A thorough investigation on the MHD natural convection flow with radioactive heat transfer past an impulsively moving plate with ramped wall temperature can be seen in [30,31]. The work on the impacts of thermal radiation and heat source on an unsteady MHD free convection flow past an infinite vertical plate including thermal diffusion has been discussed in [32,33]. The effect of Soret and radiation on transient MHD free convection from an impulsively started infinite vertical plate was explained by N Ahmed [34]. An analytical study reported in [35] investigates how Soret and Dufour effects influence mixed convective mass transfer flow past an infinite vertical porous plate. N. Ahmed et al. [36] explored the unsteady MHD free convective flow over a vertical plate in a porous medium. Their study focused on how Hall currents, thermal diffusion, and the presence of a heat source affect the flow dynamics. A comparative analysis of the Atangana-Baleanu and Caputo-Fabrizio fractional derivatives illustrated by N. A. Sheikh et al. [37]. Their study was carried out within the framework of a generalized Casson fluid model including the effects of heat generation and chemical reactions on the system. Comprehensive numerical investigations on nonsingular fractional operators for MHD flow problems with variable viscosity and thermal conductivity can be found in [38]. The concept of fractional derivatives without a singular kernel, introduced by Michele Caputo and Mauro Fabrizio [39], indicates a significant trend in fractional calculus. Traditional fractional derivatives usually consist of singular kernels, making their application difficult in science and technology. By introducing a non-singular kernel, CF approach allows a more accessible interpretation and application of fractional derivatives. F.C. Lai and F.A. Kulacki [40] examined the impacts of variable viscosity on convective heat transfer. The study focused on a vertical surface in a saturated porous medium. The impacts of variable viscosity on the heat transfer process were analyzed in their work.

Motivated by these recent advancements, we aim to investigate the effects of variable viscosity and thermal conductivity on unsteady MHD flow using non-singular fractional operator.

2. Mathematical Formulation

An unsteady MHD fluid flow over an infinite vertical surface within a porous medium that exhibits varying temperatures has been investigated. This analysis focuses on how the flow dynamics are affected by the presence of both the magnetic field and the temperature gradient in the medium. A magnetic field with uniform strength B_o is applied at a right angle to the flow direction. As shown in the figure 1, the X-axis is oriented vertically upward along the plate, while the Y-axis is positioned perpendicular to the applied magnetic field. Initially, both the liquid and the plate are at a uniform temperature $\tilde{T}_\infty$ and concentration level $\tilde{C}_\infty$. The plate accelerates exponentially with a velocity defined as $\tilde{U} = v_0\ exp(\tilde{a}t')$, when $t' > 0$.

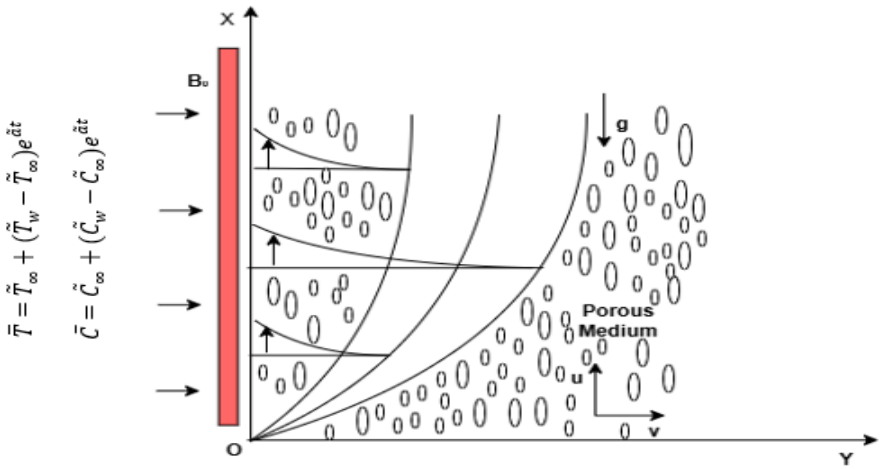

Figure 1: Fluid flow diagram

This flow configuration adheres to the condition of incompressibility. Based on the Boussinesq approximation, the governing equations and boundary conditions are as bellow:

$$\frac{\partial \tilde{U}}{\partial t'} = -\frac{\sigma\beta_0\tilde{U}}{\rho} + g\overline{\beta}(\overline{T} - \tilde{T}_\infty) + g\beta_{c'}(\overline{C} - \tilde{C}_\infty) + \nu\frac{\partial^2\tilde{U}}{\partial\tilde{y}^2} + \frac{\partial\nu}{\partial\tilde{y}}\frac{\partial\tilde{U}}{\partial\tilde{y}} - \frac{\nu\tilde{U}}{K^*}, \tag{2.1}$$

$$\rho C_p\frac{\partial\overline{T}}{\partial t'} = \lambda\frac{\partial^2\overline{T}}{\partial\tilde{y}^2} + \frac{\partial\lambda}{\partial\tilde{y}}\frac{\partial\overline{T}}{\partial\tilde{y}}, \tag{2.2}$$

$$\frac{\partial\overline{C}}{\partial t'} = D_M\frac{\partial^2\overline{C}}{\partial\tilde{y}^2} + D_T\frac{\partial^2\overline{T}}{\partial\tilde{y}^2} \tag{2.3}$$

Boundary conditions:

$$\text{For} \quad t' \leq 0 : \tilde{U} = 0, \quad \overline{T} = \tilde{T}_\infty, \quad \overline{C} = \tilde{C}_\infty, \quad \text{for all} \quad \tilde{y} < 0, \tag{2.4}$$

$$\text{For} \quad t' > 0 \quad \text{at} \quad \tilde{y} = 0 :$$

$$\tilde{U} = v_0 e^{a't'}, \quad \overline{T} = \tilde{T}_\infty + (\tilde{T}_w - \tilde{T}_\infty)e^{a't'}, \quad \overline{C} = \tilde{C}_\infty + (\tilde{C}_w - \tilde{C}_\infty)e^{a't'}, \tag{2.5}$$

$$\text{As} \quad \tilde{y} \to \infty : \tilde{U} \to 0, \quad \overline{T} \to \tilde{T}_\infty, \quad \overline{C} \to \tilde{C}_\infty \tag{2.6}$$

where $\tilde{U}$ is the fluid velocities in the X direction.

Following are the non dimensional parameters:

$$Sc = \frac{\nu_\infty}{D_M}, u = \frac{\tilde{U}}{v_0}, \quad t = \frac{t' v_0^2}{\nu_\infty}, \quad y = \frac{\tilde{y} v_0}{\nu_\infty}, \quad G_r = \frac{g\overline{\beta}(\tilde{T}_w - \tilde{T}_\infty)\nu_\infty^2}{v_0^3}, \quad G_c = \frac{g\beta_c(\tilde{C}_w - \tilde{C}_\infty)\nu_\infty^2}{v_0^3},$$
$$\theta = \frac{\overline{T} - \tilde{T}_\infty}{\tilde{T}_w - \tilde{T}_\infty}, \quad P_r = \frac{\nu_\infty C_p}{\lambda_\infty}, \quad M = \frac{\sigma B_0^2 \nu_\infty}{\rho v_0^2}, \quad \phi = \frac{\overline{C} - \tilde{C}_\infty}{\tilde{C}_w - \tilde{C}_\infty},$$
$$a = \frac{a'\nu_\infty}{v_0^2}, \quad K = \frac{v_0^2 K^*}{\nu_\infty^2}, \quad S_r = \frac{D_T(\tilde{T}_w - \tilde{T}_\infty)}{\nu_\infty(\tilde{C}_w - \tilde{C}_\infty)} \tag{2.7}$$

Thermal conductivity and viscosity of the fluid flow decrease as its temperature increases and this relationship is inversely proportional, i.e

$$\frac{1}{\mu} = \frac{1}{\mu_\infty}(1 + \gamma(\overline{T} - \tilde{T}_\infty)), \tag{2.8}$$

$$and \qquad \frac{1}{\lambda} = \frac{1}{\lambda_\infty}(1 + \delta(\overline{T} - \tilde{T}_\infty)). \tag{2.9}$$

where the constants γ and δ are related to the thermal properties of the fluid. We introduce two parameters, one is viscosity parameter $\theta_r = \frac{\tilde{T}_r - \tilde{T}_\infty}{\tilde{T}_w - \tilde{T}_\infty}$ and another is thermal conductivity parameter $\theta_c = \frac{\tilde{T}_c - T_\infty}{\tilde{T}_w - \tilde{T}_\infty}$. By applying these two parameters to equations (2.8) and (2.9), we obtain expressions for viscosity and thermal conductivity, respectively as

$$\mu = -\frac{\mu_\infty \theta_r}{\theta - \theta_r} \quad and \quad \lambda = -\frac{\lambda_\infty \theta_c}{\theta - \theta_c} \tag{2.10}$$

Using the transformation (2.7) and (2.10), the non-dimensional forms of (2.1), (2.2), and (2.3) are

$$\frac{\partial u}{\partial t} = -M^2 + G_r + G_c\phi + \frac{\theta_r}{(\theta - \theta_r)^2} \cdot \frac{\partial \theta}{\partial y}\frac{\partial u}{\partial y} - \left(\frac{\theta_r}{\theta - \theta_r}\right)\frac{\partial^2 u}{\partial y^2} + \left(\frac{\theta_r}{\theta - \theta_r}\right)\frac{u}{K}, \tag{2.11}$$

$$\frac{\partial \theta}{\partial t} = \frac{1}{Pr}\left(\frac{\theta_c}{\theta - \theta_c}\right)\left[\left(\frac{1}{\theta - \theta_c}\right)\left(\frac{\partial \theta}{\partial y}\right)^2 - \frac{\partial^2 \theta}{\partial y^2}\right], \tag{2.12}$$

$$\frac{\partial \phi}{\partial t} = \frac{1}{S_c}\left(\frac{\theta_r}{\theta - \theta_r}\right)\left[\left(\frac{1}{\theta - \theta_r}\right)\frac{\partial \phi}{\partial y}\frac{\partial \theta}{\partial y} - \frac{\partial^2 \phi}{\partial^2 y}\right] \tag{2.13}$$

With boundary conditions,

$$\text{When } t \leq 0: \quad u = 0, \theta = 0, \phi = 0 \quad \text{for all} \quad y < 0, \tag{2.14}$$

$$\text{When } t > 0: \quad u = e^{at}, \theta = e^x, \phi = e^{at} \quad \text{at} \quad y = 0, \tag{2.15}$$

$$\text{As } y \to \infty: \quad u, \quad \theta, \quad \phi \to 0 \tag{2.16}$$

Here, $M = \frac{\sigma B_0^2 \nu}{\rho v_0^2}$ is the magnetic field parameter, Sc is the Schmidt number of the fluid, G_r is the Grashof number, G_c is the concentration buoyancy parameter and the Prandtl number is given by Pr.

3. Atangana-Baleanu Fractional Derivatives Model

The AB fractional model is generated by replacing the governing time-based partial differential equations with the AB fractional operator of order α, where α is strictly lies in between 0 and 1. Equations

(2.11),(2.12), and (2.13) become,

$$AB\left(\frac{\partial^{\alpha}u(y,t)}{\partial t^{\alpha}}\right)=-M+G_r\theta+G_c\theta-\left(\frac{\theta_r}{\theta-\theta_r}\right)\frac{\partial^2 u}{\partial y^2}+\frac{\theta_r}{(\theta-\theta_r)^2}\frac{\partial u}{\partial y}\frac{\partial \theta}{\partial y}+\left(\frac{\theta}{\theta-\theta_r}\right)\frac{u}{K}, \tag{3.1}$$

$$AB\left(\frac{\partial^{\alpha}\theta(y,t)}{\partial t^{\alpha}}\right)=\frac{\theta_c}{P_r(\theta-\theta_c)}\left[\frac{1}{(\theta-\theta_c)}\left(\frac{\partial\theta}{\partial y}\right)^2-\frac{\partial^2\theta}{\partial y^2}\right], \tag{3.2}$$

$$AB\left(\frac{\partial^{\alpha}\phi(y,t)}{\partial t^{\alpha}}\right)=\frac{1}{S_c}\left[\frac{\theta_r}{(\theta-\theta_r)^2}\frac{\partial\phi}{\partial y}\frac{\partial\theta}{\partial y}-\frac{\theta}{(\theta-\theta_r)}\frac{\partial^2\phi}{\partial y^2}\right]+S_r\left[\frac{\theta_r}{(\theta-\theta_r)^2}\left(\frac{\partial\theta}{\partial y}\right)^2-\frac{\theta_r}{(\theta-\theta_r)}\frac{\partial^2\theta}{\partial y^2}\right]. \tag{3.3}$$

Where, $\frac{\partial^{\alpha}u(y,t)}{\partial t^{\alpha}}$ is the AB fractional operator of order α defined by

$$AB\left(\frac{\partial^{\alpha}(y,t)}{\partial t^{\alpha}}\right)=\frac{1}{1-\alpha}\int_0^t u'(y,t)E_{\alpha}\left(\frac{-\alpha(z-t)}{1-\alpha}\right)dt. \tag{3.4}$$

Where, $E_{\alpha}(-t^{\alpha})=\sum_{m=0}^{\infty}\frac{(-1)^{\alpha}m}{\Gamma(1+\alpha m)}$ is the Mittag-Leffler function.

4. Caputo-Fabrizio fractional derivatives Model

The CF fractional model is generated by replacing the governing time-based partial differential equations involving the CF fractional operator of order β, where β is strictly lies in between 0 and 1. (2.11),(2.12), and (2.13) become,

$$CF\left(\frac{\partial^{\beta}u(y,t)}{\partial t^{\beta}}\right)=-M+G_r\theta+G_c\theta-\left(\frac{\theta_r}{\theta-\theta_r})\right)\frac{\partial^2 u}{\partial y^2}+\frac{\theta_r}{(\theta-\theta_r)^2}\frac{\partial u}{\partial y}\frac{\partial \theta}{\partial y}+\left(\frac{\theta}{\theta-\theta_r}\right)\frac{u}{K}, \tag{4.1}$$

$$CF\left(\frac{\partial^{\beta}\theta(y,t)}{\partial t^{\beta}}\right)=\frac{\theta_c}{P_r(\theta-\theta_c)}\left[\frac{1}{(\theta-\theta_c)}\left(\frac{\partial\theta}{\partial y}\right)^2-\frac{\partial^2\theta}{\partial y^2}\right], \tag{4.2}$$

$$CF\left(\frac{\partial^{\beta}\phi(y,t)}{\partial t^{\beta}}\right)=\frac{1}{S_c}\left[\frac{\theta_r}{(\theta-\theta_r)^2}\frac{\partial\phi}{\partial y}\frac{\partial\theta}{\partial y}-\frac{\theta}{(\theta-\theta_r)}\frac{\partial^2\phi}{\partial y^2}\right]+S_r\left[\frac{\theta_r}{(\theta-\theta_r)^2}\left(\frac{\partial\theta}{\partial y}\right)^2-\frac{\theta_r}{(\theta-\theta_r)}\frac{\partial^2\theta}{\partial y^2}\right]. \tag{4.3}$$

Where, $\frac{\partial^{\beta}u(y,t)}{\partial t^{\beta}}$ represents the Caputo-Fabrizio fractional derivative of order β, as defined by

$$CF\left(\frac{\partial^{\beta}u(y,t)}{\partial t^{\beta}}\right)=\frac{1}{1-\beta}\int_0^t u'(y,t)Exp\left(\frac{-\beta(z-t)}{1-\beta}\right)dt. \tag{4.4}$$

5. Numerical solution

To solve equations (3.1)-(3.4) or (4.1)-(4.4), the ordinary finite difference method is applied, with discretization through the following formulae (5.1):

$$\frac{\partial u}{\partial t}=\frac{u_{i+1,j}-u_{i,j}}{dt},\quad \frac{\partial\theta}{\partial t}=\frac{\theta_{i+1,j}-\theta_{i,j}}{dt},\quad \frac{\partial\phi}{\partial t}=\frac{\phi_{i+1,j}-\phi_{i,j}}{dt},\quad \frac{\partial u}{\partial y}=\frac{u_{i,i+1}-u_{i,j}}{dy},\frac{\partial\theta}{\partial y}=\frac{\theta_{i,j+1}-\theta_{i,j}}{dy},$$
$$\frac{\partial\phi}{\partial y}=\frac{\phi_{i,j+1}-\phi_{i,j}}{dy},\quad \frac{\partial^2 u}{\partial y^2}=\frac{u_{i,j+1}-2u_{i,j}+u_{i,j-1}}{dy^2},\frac{\partial^2\theta}{\partial y^2}=\frac{\theta_{i,j+1}-2\theta_{i,j}+\theta_{i,j-1}}{dy^2},$$
$$\frac{\partial^2\phi}{\partial y^2}=\frac{\phi_{i,j+1}-2\phi_{i,j}+\phi_{i,j-1}}{dy^2}\ldots\quad etc. \tag{5.1}$$

Equations (3.4) or (4.4) is computed using numerical integration. Subsequently, equations (3.1)-(3.3) or (4.1)-(4.3), along with boundary conditions (2.14), (2.15), and (2.16) are discretized and solved using an

iterative Gauss-Seidel scheme. So, this boundary conditions are expressed as follows :

$$t \leq 0: \quad u_{i,j} = 0, \quad \theta_{i,j} = 0, \quad \phi_{i,j} = 0 \quad \text{for all} \quad y_{i,j} < 0, \tag{5.2}$$

$$t > 0: \quad u_{i,j} = e^{at}, \quad \theta_{i,j} = e^{x}, \quad \phi_{i,j} = e^{at} \quad \text{at} \quad y_{i,j} = 0, \tag{5.4}$$

$$u \to 0, \quad \theta_{i,j} \to 0, \quad \phi_{i,j} \to 0 \quad \text{as} \quad y_{i,j} \to \infty \tag{5.5}$$

6. Some Useful Physical Parameters

(i) Coefficient of skin friction: $C_f = \frac{\tau}{\rho v_0^2} = -\frac{\theta_r}{\theta - \theta_r}\frac{\partial u}{\partial y}\Big)_{y=0} = -\frac{\theta_r}{e^{at}-\theta_r}\left(\frac{u_{i,j}-e^{at}}{dy}\right)$, where C_f is non-dimensional skin friction. The plate is being acted upon by C_f along the free stream and $\tau(\text{viscous drag}) = \mu\frac{\partial \tilde{U}}{\partial \tilde{y}}\Big)_{\tilde{y}=0} = \mu\frac{v_0^2}{\nu}\frac{\partial u}{\partial y}\Big)_{y=0}$.

(ii) Nusselt number: $Nu = \frac{q}{\rho v_0 C_p(\tilde{T}_w - \tilde{T}_\infty)} = \frac{1}{P_r}\frac{\theta_c}{(\theta-\theta_c)}\frac{\partial \theta}{\partial y}\Big)_{y=0} = \frac{1}{P_r}\frac{\theta_c}{(\theta-\theta_c)}\left(\frac{\theta_{i,2}-e^{at}}{dy}\right)$, where Nu is Nusselt Number and $q = -\lambda\dfrac{\partial \overline{T}}{\partial \tilde{y}}$ is the heat transfer rate from the plate to the fluid.

(iii) Sherwood Number:

The mass flux q_m is in the form $q_m = -D_M\frac{\partial \overline{C}}{\partial \tilde{y}}\Big)_{\tilde{y}=0} = \frac{v_0(\tilde{C}_w - \tilde{C}_\infty)}{S_c}\frac{\theta_r}{(\theta-\theta_r)}\frac{\partial \phi}{\partial y}\Big)_{y=0}$.

The Sherwood number is $Sh = \frac{1}{S_c}\frac{\theta_r}{(e^{at}-\theta_r)}\left(\frac{\phi_{i,2}-e^{at}}{dy}\right)$.

7. The Outcomes and the Discussion

Both the AB and CF fractional derivative methods have been used in order to solve the non-dimensional discretized governing equations as well as the non-dimensional boundary conditions(5.2)-(5.5). Through the development of an appropriate MATLAB code, the necessary calculations have been carried out thoroughly and successfully. This study investigates how parameters like α, β, θ_r, θ_c, M, Pr, Sr,Gc,Gr Sc, K etc influence on velocity(u), temperature(θ), and concentration(ϕ) profiles.

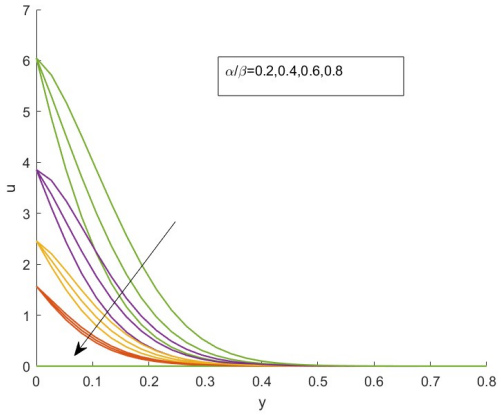

Figure 2: ***Impact of*** α & β ***on velocity***

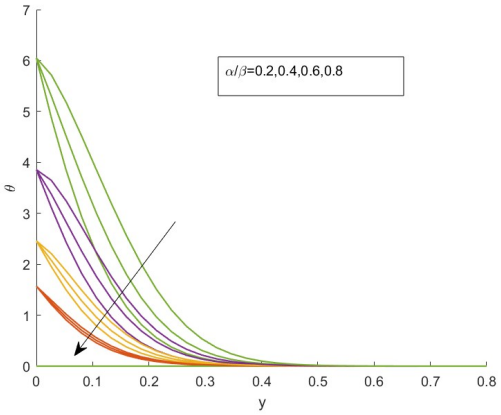

Figure 3: ***Impact of*** α & β ***on temperature***

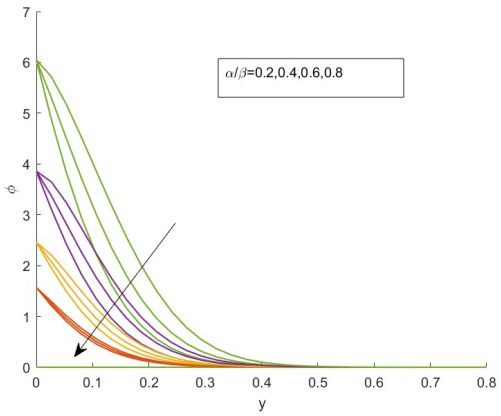

Figure 4: ***Impact of*** α & β ***on concentration***

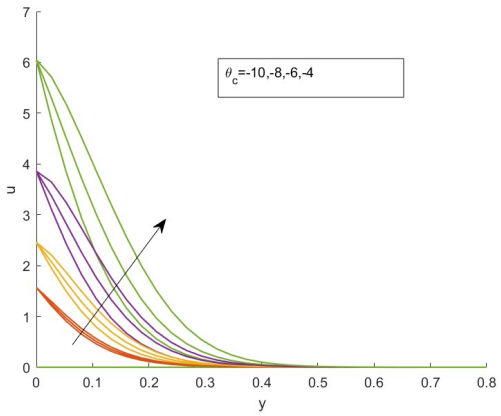

Figure 5: θ_c***'s impact on velocity***

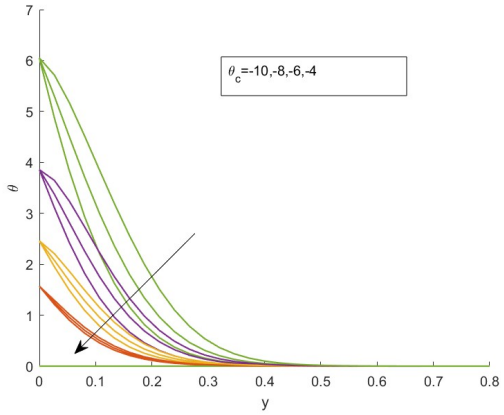

Figure 6: θ_c*'s impact on temperature*

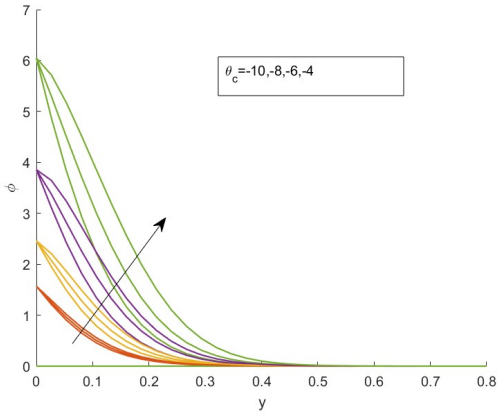

Figure 7: θ_c*'s impact on concentration*

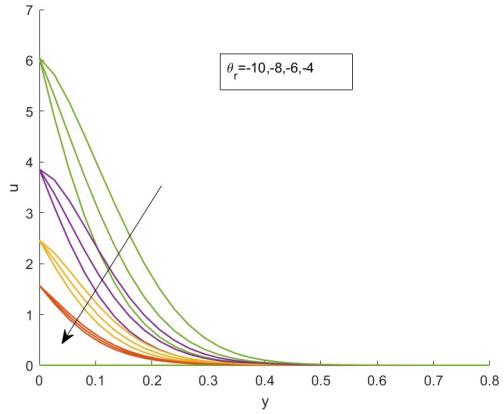

Figure 8: θ_r*'s impact on velocity*

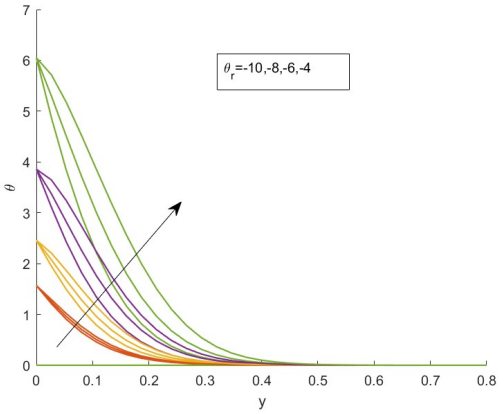

Figure 9: θ_r*'s impact on temperature*

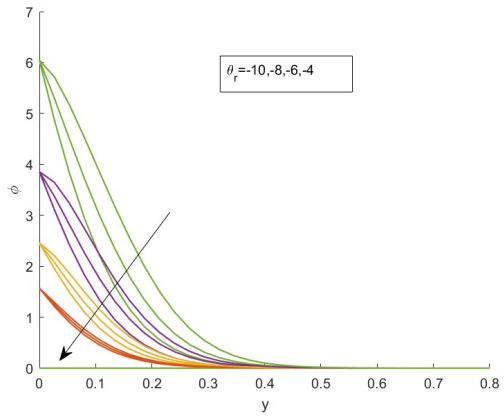

Figure 10: θ_r*'s impact on concentration*

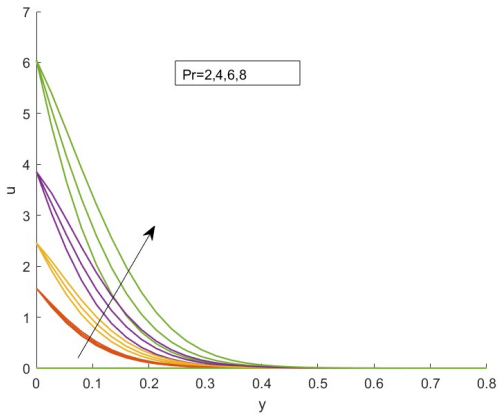

Figure 11: ***Pr's impact on velocity***

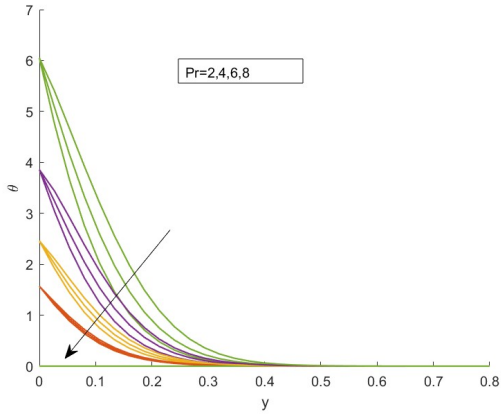

Figure 12: ***Pr's impact on temperature***

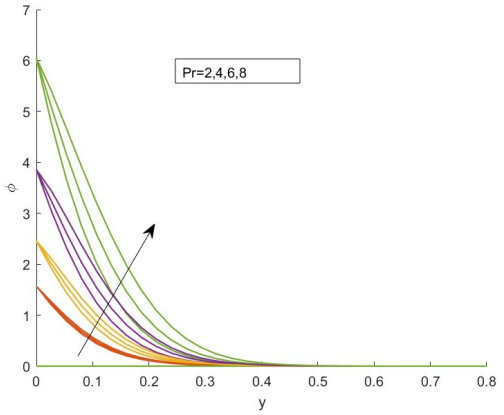

Figure 13: ***Pr's impact on concentration***

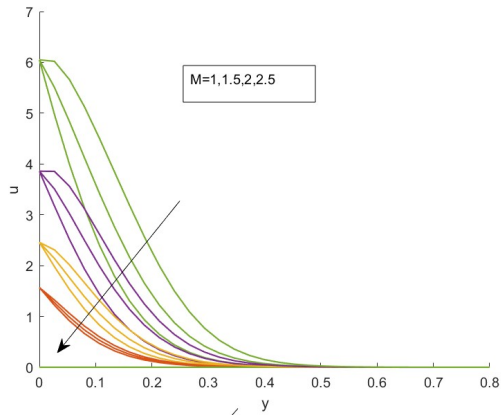

Figure 14: ***M's impact on velocity***

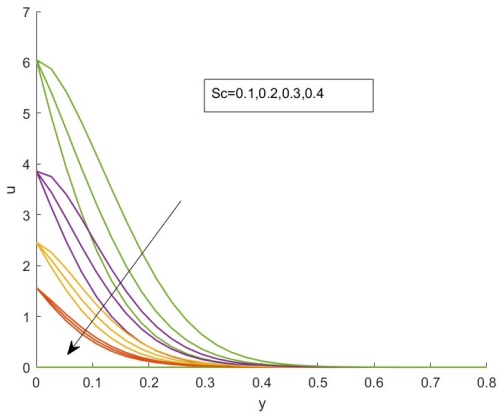

Figure 15: ***Sc's impact on velocity***

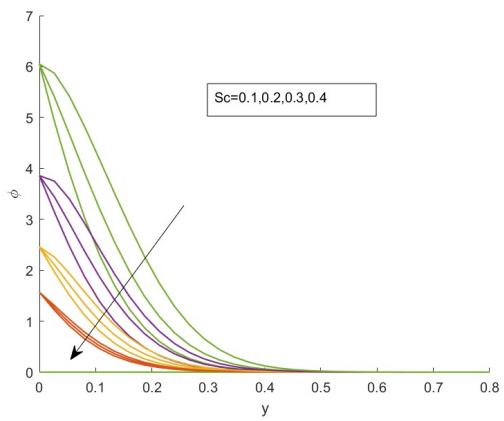

Figure 16: ***Sc's impact on concentration***

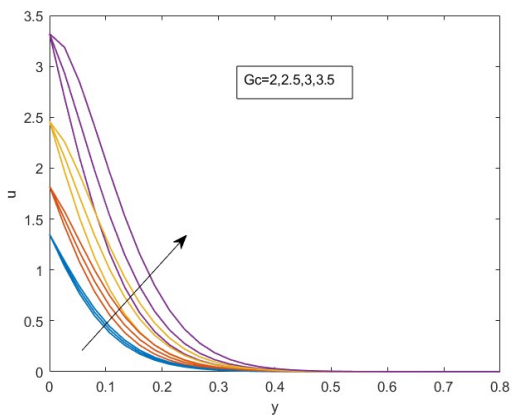

Figure 17: *Gc*'s impact on velocity***

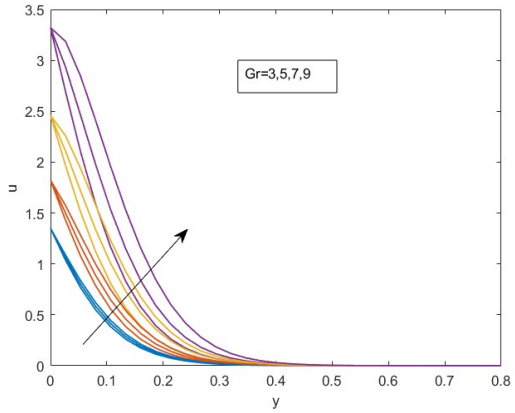

Figure 18: *Gr's impact on velocity*

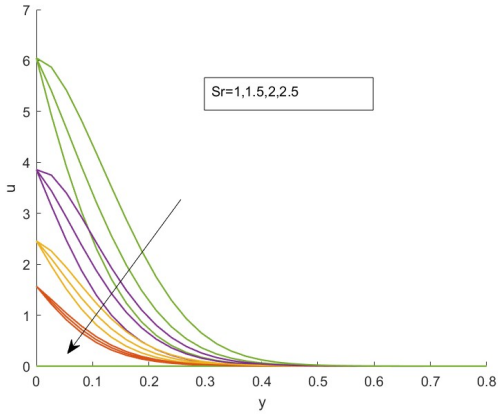

Figure 19: ***Sr's impact on velocity***

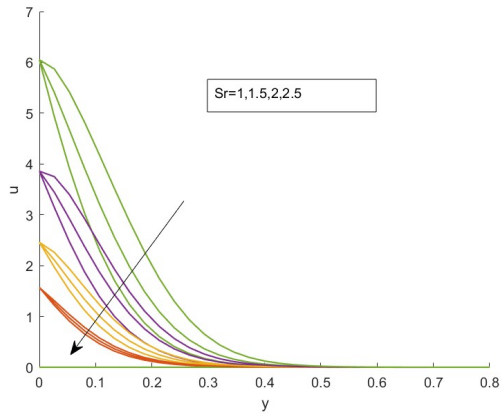

Figure 20: ***Sr's impact on concentration***

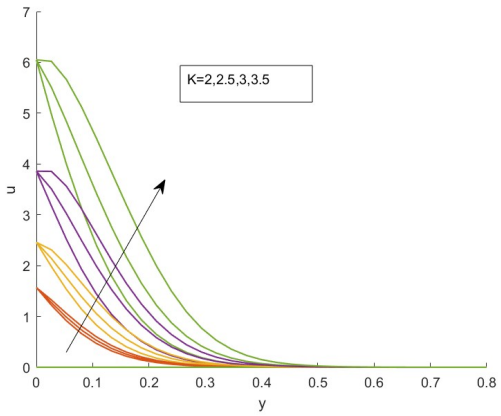

Figure 21: *K's impact on velocity*

For different values of α & β, the velocity, temperature, and concentration profile are illustrated in figures 2, 3, and 4 receptively. Here the figures indicating that the profiles of velocity(u), temperature(θ), and concentration (ϕ) decrease while the value of α & β rise. The θ_c's effects on velocity, temperature, and concentration are demonstrated in figures 5, 6, and 7 respectively, indicating that both velocity and concentration increase as θ_c increases, while temperature shows an downward trend with rising values of θ_c. As illustrated in figures 8, 9, and 10 respectively, the θ_r's impacts on velocity, temperature, and concentration reveal a decline in both velocity and concentration profile with higher θ_r's values, whereas temperature increases as θ_r rises. In figure 11, 12, and 13 respectively, the Pr's impacts on velocity(u), temperature(θ), and concentration (ϕ) profiles are evident, with velocity and concentration increasing in response to increasing Pr, while temperature shows a negative correlation with Pr. Figure 14 illustrated the influence of M on velocity(u) profiles, indicating that the velocity profile exhibits an increasing trend with higher values of M. The variations of velocity and concentration profiles with respect to different Sc values are illustrated in figures 15, and 16 respectively, indicating that both profiles decline as Sc increases. Based on figure 17, it is seen that the rise in Gc is associated with increases in velocity profiles. Figure 18 displays the variation of velocity profile for various values of Gr. Here the velocity profile increases with increasing value of Gr. In Figures 19, and 20 respectively, it is observed that an increase in Sr leads to decreases in Velocity and concentration profile. The impacts of increasing K on the Velocity

profile are displayed in 21, showing an upward trend in the velocity profile.

8. A comparative analysis of the AB and CF fractional derivatives

Under different parameters the AB and CF fractional derivative methods are evaluated and compared which are elaborately demonstrated in the tables 1-7 . The velocity, temperature and concentration profiles for different values of parameter are nearly identical when comparing the AB and CF fractional derivatives. However, the values for the CF method are slightly lower than those of the AB method for u, θ and ϕ.

Table 1: α/β's impact on u, θ and ϕ

$\alpha/\beta \rightarrow$		0.2			0.4			0.6		
$t \rightarrow$		0.4	0.8	1.2	0.4	0.8	1.2	0.4	0.8	1.2
u	AB	0.234373	0.311907	0.41337	0.234335	0.311798	0.413135	0.234301	0.311694	0.412907
	CF	0.234999	0.313586	0.416715	0.235054	0.313753	0.417069	0.235123	0.31397	0.417555
θ	AB	0.238704	0.320565	0.429848	0.238676	0.320484	0.429669	0.238651	0.320406	0.429494
	CF	0.238777	0.320767	0.430262	0.238762	0.320725	0.430174	0.23875	0.320695	0.430114
ϕ	AB	0.236986	0.317551	0.424583	0.236979	0.317529	0.424536	0.236972	0.317508	0.42449
	CF	0.237118	0.317911	0.425319	0.23713	0.317948	0.425399	0.237145	0.317996	0.425507

Table 2: θ_c's impact on u,θ and ϕ

$\theta_c \rightarrow$		-10			-8			-6		
t $\rightarrow$		0.4	0.8	1.2	0.4	0.8	1.2	0.4	0.8	1.2
u	AB	0.175656	0.233159	0.307955	0.175676	0.233205	0.308058	0.175708	0.233278	0.308217
	CF	0.176218	0.234704	0.31109	0.176238	0.234749	0.31119	0.17627	0.23482	0.311344
θ	AB	0.237979	0.319246	0.427505	0.236979	0.317507	0.424522	0.235377	0.314755	0.419866
	CF	0.238071	0.31951	0.428064	0.237071	0.317771	0.425082	0.23547	0.315019	0.420427
ϕ	AB	0.236987	0.317545	0.424572	0.237005	0.317584	0.424655	0.237033	0.317645	0.424784
	CF	0.237149	0.317997	0.425507	0.237167	0.318036	0.42559	0.237195	0.318096	0.425718

Table 3: θ_r's on u,θ and ϕ

$\theta_r \rightarrow$		-10			-8			-6		
t $\rightarrow$		0.4	0.8	1.2	0.4	0.8	1.2	0.4	0.8	1.2
u	AB	0.173976	0.230237	0.302944	0.171551	0.22607	0.295901	0.167695	0.219535	0.285045
	CF	0.174532	0.231762	0.306029	0.172098	0.227565	0.298915	0.168229	0.220986	0.287954
θ	AB	0.238663	0.320445	0.429582	0.238674	0.320455	0.429596	0.238683	0.320465	0.429623
	CF	0.238756	0.320708	0.430141	0.238766	0.320718	0.430152	0.238776	0.320735	0.430165
ϕ	AB	0.235964	0.315753	0.421472	0.234485	0.313194	0.417105	0.23212	0.309146	0.410302
	CF	0.236126	0.316206	0.422411	0.234648	0.313648	0.41805	0.232283	0.309604	0.411258

Table 4: Pr's impact on u,θ and ϕ

$Pr \rightarrow$		2			4			6		
$t \rightarrow$		0.4	0.8	1.2	0.4	0.8	1.2	0.4	0.8	1.2
u	AB	0.175673	0.233247	0.308222	0.175706	0.233363	0.308543	0.175736	0.233479	0.308876
	CF	0.175655	0.232683	0.305753	0.175083	0.230606	0.300259	0.174508	0.228512	0.294726
θ	AB	0.236657	0.31463	0.417053	0.234593	0.308704	0.404414	0.232546	0.302878	0.392129
	CF	0.239301	0.322188	0.433113	0.239893	0.323879	0.436758	0.240511	0.325736	0.441015
ϕ	AB	0.237003	0.31762	0.424789	0.237032	0.317725	0.425076	0.237061	0.317829	0.425356
	CF	0.237093	0.317817	0.425063	0.237047	0.317653	0.424637	0.237	0.317481	0.424185

Table 5: M's impact on u & Sc's impact on u and ϕ

M	t	u		Sc	t	u		ϕ	
		AB	CF			AB	CF	AB	CF
1.1	0.4	0.238872	0.239649	0.1	0.4	0.17564	0.176212	0.236838	0.237658
	0.8	0.317886	0.320019		0.8	0.233121	0.234695	0.31718	0.319478
	1.2	0.4213	0.425621		1.2	0.307871	0.311067	0.423819	0.428601
1.6	0.4	0.237328	0.238101	0.2	0.4	0.175636	0.176221	0.236666	0.23831
	0.8	0.315814	0.317933		0.8	0.233113	0.234722	0.316758	0.321371
	1.2	0.418523	0.422815		1.2	0.307855	0.311126	0.422953	0.43257
2.1	0.4	0.235797	0.236564	0.3	0.4	0.175633	0.17623	0.236495	0.238964
	0.8	0.313759	0.315864		0.8	0.233105	0.23475	0.316336	0.323274
	1.2	0.415768	0.420032		1.2	0.307839	0.311185	0.422089	0.436573

Table 6: K's impact on u & Sr's impact on u and ϕ

K	t	u		Sr	t	u		ϕ	
		AB	CF			AB	CF	AB	CF
2.1	0.4	0.175437	0.175998	1	0.4	0.23431	0.235078	0.235646	0.235787
	0.8	0.232856	0.234399		0.8	0.311732	0.313839	0.315174	0.315566
	1.2	0.307526	0.310659		1.2	0.412996	0.417265	0.420396	0.421202
2.6	0.4	0.175488	0.17605	1.5	0.4	0.234306	0.235074	0.234974	0.235106
	0.8	0.232923	0.234467		0.8	0.311725	0.313832	0.313988	0.314351
	1.2	0.307615	0.310749		1.2	0.412983	0.417252	0.418315	0.419057
3.1	0.4	0.175522	0.176084	2	0.4	0.234302	0.23507	0.234302	0.234424
	0.8	0.232969	0.234513		0.8	0.311717	0.313825	0.312803	0.313137
	1.2	0.307675	0.310809		1.2	0.412971	0.417239	0.416233	0.416912

Table 7: Impression of Gr and Gc on u

Gr	t	u		Gc	u	
		AB	CF		AB	CF
3	0.4	0.175642	0.176204	2	0.16982	0.170374
	0.8	0.233127	0.234673		0.22528	0.22679
	1.2	0.307884	0.31102		0.29729	0.300362
5	0.4	0.176292	0.176855	2.5	0.17047	0.171022
	0.8	0.234005	0.235554		0.22615	0.227666
	1.2	0.309071	0.312214		0.29847	0.301546
7	0.4	0.176942	0.177506	3	0.17112	0.17167
	0.8	0.234883	0.236435		0.22702	0.228542
	1.2	0.310258	0.313408		0.29964	0.302731

9. A comparison between AB and CF fractional derivative under different parameter i.e C_f, Nu and Sh.

Considering the values of $\alpha = 0.25$ and $\beta = 0.5$, the values for C_f, Nu and Sh are calculated using both AB and CF method under different parameters. The variation of coefficient of skin friction, Nusselt Number and Sherwood number against different parameters are demonstrated in the table 8 and table 9 respectively . It is observed that the Nu and Sh increase for the rising value of θ_c and C_f increases with the increasing value of θ_r.

Table 8: Table for Nu and Sh

α / β	θ_c	Nu		Sh	
		AB	CF	AB	CF
0.25	-12	0.000993	0.000992	5.479864	5.448328
	-10	0.006138	0.006129	5.478339	5.446816
	-8	0.036482	0.036432	5.476134	5.444631
	-6	0.203948	0.203664	5.472664	5.441195
0.5	-12	0.000993	0.000992	5.48676	5.447348
	-10	0.00614	0.00613	5.485231	5.445836
	-8	0.036498	0.036437	5.48302	5.443651
	-6	0.20404	0.203691	5.479542	5.440214

Table 9: Table for C_f and Sh

α/ β	θ_r	C_f		Sh	
		AB	CF	AB	CF
0.25	-12	-0.000702	-0.0007	7.479864	7.448328
	-10	-0.004353	-0.004342	6.609313	5.578135
	-8	-0.025989	-0.025924	5.353712	5.323038
	-6	-0.146278	-0.145918	5.384797	5.35488
0.5	-12	-0.000703	-0.0007	5.48676	5.447348
	-10	-0.004356	-0.004342	5.616127	5.577136
	-8	-0.026005	-0.025923	5.360413	5.322012
	-6	-0.146365	-0.145916	5.391328	5.353815

10. Conclusion

Based on the above study, it can be concluded as follows: The study provides a numerical approach to analyze the impact of different parameters on MHD flow past an inclined vertical plate using the AB and CF fractional derivatives.

(i) Impact of fractional derivative parameters (α & β): As the parameters α and β increase, both the velocity and temperature profiles decrease, as shown in table 1.

(ii) Magnetic field parameter (M): Increasing the value of M results in a decline in velocity profile, as demonstrated in table 5.

(iii) Thermal Grashof Number (Gr) and Concentration Grashof Number (Gc): Table 7 indicates that When both Gr and Gm increase, the velocity profile rises.

(iv) Variable viscosity (θ_r) and thermal conductivity (θ_c): An increase in θ_r enhances the temperature profile, but decrease in velocity and concentration profiles. On the other hand, both velocity and concentration increases but temperature decreases with the increasing value of θ_c, as illustrated in table 1 and 2 respectively.

(v) Schmidt Number (Sc) and Soret Number (Sr): As Sc and Sr increase, both velocity and concentration diminish, but the temperature profile shows an upward trend, as shown in tables 5 and 6 respectively.
(vi) Prandtl Number (Pr): When Pr increases, both velocity and temperature increase, while concentration shows an downward trend, as seen in table 4.
(vii) Permeability Parameter (K): Table 6 illustrates that the velocity profile increases as K grows. Finally, the velocity, temperature, and concentration profiles have been examined for different parameters. The results show that the values obtained using both AB and CF fractional derivatives are nearly identical.

11. Terminology

Table 10: Nomenclature

Symbol	Description	Symbol	Description
$\vec{q}$	Fluid velocity	$\tilde{T}_w$	Wall temperature
$\vec{B}$	Density of magnetic field	$\tilde{T}_\infty$	Fluid temperature (distant from the plate)
$\vec{J}$	Current density vector(A/m2)	K_T	Thermal diffusion ratio
λ	Thermal conductivity	D_M	Mass diffusivity
B_0	Applied magnetic field (weber/m^2)	$\overline{C}$	Species concentration
t	Time (s)	$\tilde{C_w}$	Wall concentration
$\tilde{a}$	Accelerating parameter	$\tilde{C}_\infty$	Concentration (distant from the plate)
ν_0	Suction velocity	U_0	Velocity of the plate
C_p	Specific heat(constant pressure)	ρ	Fluid density
M	Magnetic parameter	μ	Coefficient of viscosity
Pr	Prandtl number	σ	Electrical conductivity
Sc	Schmidt number	κ	Thermal conductivity
D_T	Thermal diffusion coefficient	ν	Kinematic viscosity
Sr	Soret number	$\overline{\beta}$	Volumetric coefficient of thermal expansion
Gr	Thermal Grashof number	$\beta_{c'}$	Volumetric coefficient (solutal expansion)
Gc	Mass Grashof number	θ	Dimensionless temperature
$\overline{T}$	Fluid temperature	ϕ	Dimensionless concentration
K	Non-dimensional Permeability	K^*	Dimensional Permeability of the Porous Medium
$\tilde{U}$	dimensional velocity	g	acceleration due to gravity
u	Fluid velocity		

References

1. H. Alfvén, *Existence of electromagnetic-hydrodynamic waves*, Nature **150** (1942), no. 3805, 405–406. doi:10.1038/150405d0.
2. V. C. Ferraro and C. Plumpton, *Introduction to magneto-fluid mechanics*, 1966.
3. K. R. Cramer and S. I. Pai, *Magnetofluid dynamics for engineers and applied physicists*, 1973.
4. D. A. Nield and A. Bejan, *Convection in porous media*, vol. 3, Springer, New York, 2006.
5. P. S. Hiremath and P. M. Patil, *Free convection effects on the oscillatory flow of a couple stress fluid through a porous medium*, Acta Mech. **98** (1993), 143–158. https://doi.org/10.1007/BF01174299.
6. B. Shankar Goud, P. Srilatha, T. Srinivasulu, Y. D. Reddy, and K. S. Kumar, *Induced by heat source on unsteady MHD free convective flow of Casson fluid past a vertically oscillating plate through porous medium utilizing finite difference method*, Mater. Today Proc. (2023). https://doi.org/10.1016/j.matpr.2023.01.378.
7. N. Gulle and R. Kodi, *Soret radiation and chemical reaction effect on MHD Jeffrey fluid flow past an inclined vertical plate embedded in porous medium*, Mater. Today Proc. **50** (2022), 2218–2226.
8. A. Sandhya, G. Reddy, and G. V. S. R. Deekshitulu, *Radiation and chemical reaction effects on MHD Casson fluid flow past a semi-infinite vertical moving porous plate*, 2020. https://doi.org/10.56042/ijpap.v58i7.31001.
9. R. Srinivasa Raju, *Unsteady MHD boundary layer flow of Casson fluid over an inclined surface embedded in a porous medium with thermal radiation and chemical reaction*, J. Nanofluids **7** (2018), no. 4, 694–703. https://doi.org/10.1166/jon.2018.1500.

10. S. Srinivas, P. B. A. Reddy, and B. S. R. V. Prasad, *Effects of chemical reaction and thermal radiation on MHD flow over an inclined permeable stretching surface with non-uniform heat source/sink: An application to the dynamics of blood flow*, J. Mech. Med. Biol. **14** (2014), no. 5, 1450067. https://doi.org/10.1142/S0219519414500675.

11. E. Omamoke and E. Amos, *Chemical reaction, radiation and heat source effects on unsteady MHD blood flow over a horizontal porous surface in the presence of an inclined magnetic field*, Int. J. Sci. Eng. Res. **11** (2020), no. 4.

12. D. Pal and B. Talukdar, *Buoyancy and chemical reaction effects on MHD mixed convection heat and mass transfer in a porous medium with thermal radiation and Ohmic heating*, Commun. Nonlinear Sci. Numer. Simul. **15** (2010), no. 10, 2878–2893. https://doi.org/10.1016/j.cnsns.2009.10.029.

13. N. S. Wahid, N. M. Arifin, N. S. Khashi'ie, I. Pop, N. Bachok, and M. E. H. Hafidzuddin, *MHD mixed convection flow of a hybrid nanofluid past a permeable vertical flat plate with thermal radiation effect*, Alex. Eng. J. **61** (2022), no. 4, 3323–3333. https://doi.org/10.1016/j.cjph.2023.07.016.

14. K. Suneetha, S. M. Ibrahim, and G. V. Ramana Reddy, *The effects of radiation and chemical reaction on MHD mixed convective flow and mass transfer from a vertical surface with Ohmic heating and viscous dissipation*, Multidiscip. Model. Mater. Struct. **16** (2020), no. 1, 191–207. https://doi.org/10.1108/MMMS-02-2018-0021.

15. O. Aydın and A. Kaya, *Radiation effect on MHD mixed convection flow about a permeable vertical plate*, Heat Mass Transf. **45** (2008), 239–246. https://doi.org/10.1007/s00231-008-0428-y.

16. S. Naramgari, S. Vangala, and M. Penem, *Aligned magnetic field, radiation, and rotation effects on unsteady hydromagnetic free convection flow past an impulsively moving vertical plate in a porous medium*, Int. J. Eng. Math. (2014), no. 1, 565162. https://doi.org/10.1155/2014/565162.

17. N. Sandeep and V. Sugunamma, *Radiation and inclined magnetic field effects on unsteady hydromagnetic free convection flow past an impulsively moving vertical plate in a porous medium*, J. Appl. Fluid Mech. **7** (2014), no. 2, 275–286. https://doi.org/10.36884/jafm.7.02.19431.

18. A. Kumar, *MHD free convective fluctuating flow through a porous effect with variable permeability parameter*, Int. J. Eng. **23** (2010), no. 3, 313–322.

19. B. K. Sharma, R. C. Chaudhary, and P. K. Sharma, *Fluctuating mass transfer on three-dimensional flow through a porous medium with variable permeability*, Adv. Theor. Appl. Math. **2** (2007), no. 3, 257–267.

20. M. V. Krishna and K. Jyothi, *Heat and mass transfer on MHD rotating flow of a visco-elastic fluid through porous medium with time-dependent oscillatory permeability*, J. Anal. **27** (2019), no. 2, 643–662. https://doi.org/10.1007/s41478-018-0099-0.

21. R. N. Barik, G. C. Dash, and M. Kar, *Unsteady free convective MHD flow and mass transfer through porous medium in a rotating system with fluctuating heat source/sink and chemical reaction*, J. Appl. Anal. Comput. **4** (2014), no. 3, 231–244.

22. J. R. Pattnaik, G. C. Dash, and S. Singh, *Radiation and mass transfer effects on MHD free convection flow through porous medium past an exponentially accelerated vertical plate with variable temperature*, Ann. Fac. Eng. Hunedoara **10** (2012), no. 3, 175.

23. B. S. Goud, B. S. Babu, M. N. Raja Shekar, and G. Srinivas, *Mass transfer effects on MHD flow through porous medium past an exponentially accelerated inclined plate with variable temperature and thermal radiation*, Int. J. Thermofluid Sci. Technol. **6** (2019), 19060402. http://dx.doi.org/10.36963/IJTST.19060402.

24. G. S. Seth, R. Sharma, and B. Kumbhakar, *Heat and mass transfer effects on unsteady MHD natural convection flow of a chemically reactive and radiating fluid through a porous medium past a moving vertical plate with arbitrary ramped temperature*, J. Appl. Fluid Mech. **9** (2015), no. 1, 103–117. https://doi.org/10.18869/acadpub.jafm.68.224.23961.

25. U. S. Rajput and S. Kumar, *Radiation effects on MHD flow past an impulsively started vertical plate with variable heat and mass transfer*, Int. J. Appl. Math. Mech. **8** (2012), no. 1, 66–85.

26. A. Selvaraj and E. Jothi, *Heat source impact on MHD and radiation absorption fluid flow past an exponentially accelerated vertical plate with exponentially variable temperature and mass diffusion through a porous medium*, Mater. Today Proc. **46** (2021), 3490–3494. https://doi.org/10.1016/j.matpr.2020.11.919.

27. B. K. Taid, N. Ahmed, and S. Sarma, *Heat source and radiation absorption on unsteady MHD fluid flow over an infinite vertical plate embedded in a porous medium in presence of Soret effect*, J. Math. Comput. Sci. **11** (2021), no. 6, 7154–7169. https://doi.org/10.28919/jmcs/6149.

28. S. Sarma and N. Ahmed, *Thermal diffusion effect on unsteady MHD free convective flow past a semi-infinite exponentially accelerated vertical plate in a porous medium*, Can. J. Phys. **100** (2022), no. 10, 437–451. https://doi.org/10.1139/cjp-2021-0361.

29. S. F. Ahmmed, R. Biswas, and M. Afikuzzaman, *Unsteady magnetohydrodynamic free convection flow of nanofluid through an exponentially accelerated inclined plate embedded in a porous medium with variable thermal conductivity in the presence of radiation*, J. Nanofluids **7** (2018), no. 5, 891–901. https://doi.org/10.1166/jon.2018.1520.

30. G. S. Seth, Md S. Ansari, and R. Nandkeolyar, *MHD natural convection flow with radiative heat transfer past an impulsively moving plate with ramped wall temperature*, Heat Mass Transfer **47** (2011), 551–561. https://doi.org/10.1007/s00231-010-0740-1.

31. N. Ghara, S. Das, S. L. Maji, and R. N. Jana, *Effect of radiation on MHD free convection flow past an impulsively moving vertical plate with ramped wall temperature*, Amer. J. Sci. Ind. Res. **3** (2012), no. 6, 376–386. https://doi.org/10.5251/AJSIR.2012.3.6.376.386.

32. R. Srinivasa Raju, K. Sudhakar, and M. Rangamma, *The effects of thermal radiation and heat source on an unsteady MHD free convection flow past an infinite vertical plate with thermal diffusion and diffusion thermo*, J. Inst. Eng. (India): Ser. C **94** (2013), 175–186. https://doi.org/10.1007/s40032-013-0063-3.

33. F. S. Ibrahim, A. M. Elaiw, and A. A. Bakr, *Effect of the chemical reaction and radiation absorption on the unsteady MHD free convection flow past a semi-infinite vertical permeable moving plate with heat source and suction*, Commun. Nonlinear Sci. Numer. Simul. **13** (2008), no. 6, 1056–1066. https://doi.org/10.1016/j.cnsns.2006.09.007.

34. N. Ahmed, *Soret and radiation effects on transient MHD free convection from an impulsively started infinite vertical plate*, (2012), 062701. https://doi.org/10.1115/1.4005749.

35. N. Ahmed, *MHD convection with Soret and Dufour effects in a three-dimensional flow past an infinite vertical porous plate*, Can. J. Phys. **88** (2010), no. 9, 663–674. https://doi.org/10.1139/P10-056.

36. N. Ahmed, H. Kalita, and D. P. Barua, *Unsteady MHD free convective flow past a vertical porous plate immersed in a porous medium with Hall current, thermal diffusion and heat source*, Int. J. Eng. Sci. Technol. **2** (2010), no. 6. http://dx.doi.org/10.4314/ijest.v2i6.63699.

37. N. A. Sheikh, F. Ali, M. Saqib, I. Khan, S. A. A. Jan, A. S. Alshomrani, and M. S. Alghamdi, *Comparison and analysis of the Atangana–Baleanu and Caputo–Fabrizio fractional derivatives for generalized Casson fluid model with heat generation and chemical reaction*, Results Phys. **7** (2017), 789–800. https://doi.org/10.1016/j.rinp.2017.01.025.

38. D. Saikia, U. K. Saha, and G. C. Hazarika, *A numerical study of Atangana-Baleanu and Caputo-Fabrizio for MHD flow problem over a vertical hot stretching sheet with variable viscosity and thermal conductivity*, IAENG Int. J. Appl. Math. **50** (2020), no. 3.

39. M. Caputo and M. Fabrizio, *A new definition of fractional derivative without singular kernel*, Prog. Fract. Differ. Appl. **1** (2015), no. 2, 73–85.

40. F. C. Lai and F. A. Kulacki, *The effect of variable viscosity on convective heat transfer along a vertical surface in a saturated porous medium*, Int. J. Heat Mass Transfer **33** (1990), no. 5, 1028–1031. https://doi.org/10.1016/0017-9310(90)90084-8.

Bhaskar Jyoti Bhuyan,
Department of Basic and Applied Science,
National Institute of Technology Arunachal Pradesh,
India - 791113
Email: bjbhuyan81@gmail.com
ORCID: 0009-0002-6196-8683

Utpal Kumar Saha (Corresponding Author),
Department of Basic and Applied Science,
National Institute of Technology Arunachal Pradesh,
India - 791113
Email: uksahanitap@gmail.com
ORCID: 0000-0002-0143-1625

G.C. Hazarika,
Department of Mathematics,
Dibrugarh University, Dibrugarh, Assam, India - 786004
Email: gchazarika@gmail.com
ORCID: 0000-0003-3937-8919

Dipen Saikia,
Department of Mathematics,
Salt Brook Academy, Dibrugarh, Assam, India - 786003
Email: deepsand2009@gmail.com
ORCID: 0009-0005-9097-1824